LIMNOLOGY AND OCEANOGRAPHY
Letters

ASLO
Open Access

Limnology and Oceanography Letters 8, 2023, 359–367

doi: 10.1002/lol2.10311

LETTER

Alkalinity contributes at least a third of annual gross primary production in a deep stratified hardwater lake

Pascal Perolo [1]* *Nicolas Escoffier* [1] *Hannah E. Chmiel* [2] *Gaël Many* [1] *Damien Bouffard* [1,3] *Marie-Elodie Perga* [1]

[1]Institute of Earth Surface Dynamics, University of Lausanne, Lausanne, Switzerland; [2]Physics of Aquatic Systems Laboratory, Margareth Kamprad Chair, Swiss Federal Institute of Technology Lausanne, Lausanne, Switzerland; [3]Department of Surface Waters—Research and Management, Eawag, Swiss Federal Institute of Aquatic Science and Technology, Kastanienbaum, Switzerland

Scientific Significance Statement

If CO_2 is the main carbon-substrate for photosynthesis, how can gross primary production (GPP) carry on when surface CO_2 is depleted? In Lake Geneva, GPP can reach its highest rates when the surface CO_2 concentrations are the lowest. This suggests that photosynthetic organisms could heavily use an alternate carbon source, abundant in hardwater lakes, that is, bicarbonates. We demonstrated for the first time that bicarbonates support the GPP for two-thirds of the year. In the littoral and pelagic environments, we estimated that more than one-third of the annual primary production was ultimately provided by bicarbonate fixation. We showed that, far from being anecdotal, bicarbonate fixation by primary producers can be the most frequent model for hardwater lakes.

Abstract

In alkaline freshwater systems, the apparent absence of carbon limitation to gross primary production (GPP) at low CO_2 concentrations suggests that bicarbonates can support GPP. However, the contribution of bicarbonates to GPP has never been quantified in lakes along the seasons. To detect the origin of the inorganic carbon maintaining GPP, we analyze the daily stoichiometric ratios of CO_2–O_2 and alkalinity–O_2 in a deep hardwater lake. Results show that aquatic primary production withdraws bicarbonate from the alkalinity pool for two-thirds of the year. Alkalinity rather than CO_2 is the dominant inorganic carbon source for GPP throughout the stratified period in both the littoral and pelagic environments. This study sheds light on the neglected role of alkalinity in the freshwater carbon cycle throughout an annual cycle.

In aquatic ecosystems, gross primary production (GPP) converts dissolved inorganic carbon ($DIC = CO_2 + HCO_3^- + CO_3^{2-}$) into organic matter. Nutrients (nitrogen and phosphorus) and light are the main limiting factors of GPP (Schindler et al. 1973; Dillon and Rigler 1974; Krause-Jensen and Sand-Jensen 1998; Karlsson et al. 2009). Because additions of DIC to lakes were not sufficient to increase GPP levels (Schindler 1971, 1974), DIC

*Correspondence: pascal.perolo@gmail.com

Associate editor: Janne Karlsson

Author Contribution Statement: PP, MEP, and DB conceived the study design. PP, NE, and HEC collected and preprocessed data field. PP and MEP performed data analysis and modeling. PP, MEP, and DB drafted the manuscript with inputs from all authors.
Data Availability Statement: Data and metadata are available in the Zenodo repository at https://doi.org/10.5281/zenodo.7442327.

Additional Supporting Information may be found in the online version of this article.

limitation of GPP has been regarded as unlikely, especially since most inland waters are supersaturated with CO_2 (Cole et al. 1994). This statement has been questioned in cases of near-surface CO_2 undersaturation when GPP demand surpasses inward atmospheric CO_2 fluxes (Schindler et al. 1972; Finlay et al. 1999; Zhang et al. 2017; Zagarese et al. 2021). Under such conditions, the GPP in low-alkaline soft water lakes has been proven to be carbon-limited (Kragh and Sand-Jensen 2018).

In the same study, Kragh and Sand-Jensen (2018) did not detect any carbon limitation of GPP at such low near-surface CO_2 in high-alkaline hardwater lakes. The absence of carbon limitation was therein attributed to the high DIC stocks. However, at pH values typical for moderate hardwater lakes (7.8–9), the DIC pool is mainly composed of bicarbonates (HCO_3^- > 95%; Stumm and Morgan 1981) that cannot be readily fixed by most primary producers. At high HCO_3^- concentrations and high pH, atmospheric CO_2 invasion is greatly enhanced by chemical enhancement (Wanninkhof and Knox 1996). Yet, the carbonate buffering effect leads to fast hydration and deprotonation of incoming atmospheric CO_2 into HCO_3^- with limited effect on pH and dissolved CO_2 concentrations (Bade and Cole 2006). Thus, the chemical enhancement of atmospheric inward fluxes in alkaline lakes cannot directly supply CO_2 to primary producers. The apparent lack of carbon limitation of GPP in alkaline hardwater lakes despite low CO_2 concentrations suggests that alkalinity can deliver DIC to primary producers (Li et al. 2018).

Primary producers, inhabiting environments with low CO_2, high HCO_3^-, and high light levels (Maberly and Gontero 2017) have evolved complex strategies to use HCO_3^- for maintaining GPP (e.g., Steemann Nielsen 1946; Thomas and Tregunna 1968; Price et al. 2008; Maberly and Gontero 2017; Iversen et al. 2019). At low CO_2 concentrations, certain microalgae and cyanobacteria can mobilize active HCO_3^- uptake systems. Bicarbonate is transported to cell compartments where specific enzymes concentrate and convert HCO_3^- into CO_2 (CO_2-concentrating mechanism [CCM]; e.g., carbon anhydrase; Colman et al. 2002; Li et al. 2018). For active HCO_3^- uptake, 1 mol of alkalinity is lost as 1 mol of inorganic carbon is fixed within photosynthesis. Another mechanism to ensure carbon supply to GPP involves the capture of the CO_2 released during calcite precipitation (CP: $2HCO_3^- + Ca^{2+} \rightleftarrows CaCO_3 + CO_2 + H_2O$) that can occur close to the membranes of many algae and macrophytes (Kelts and Hsü 1978; Larsson and Axelsson 1999; Pełechaty et al. 2013; Müller et al. 2016). For indirect HCO_3^- use through CP, 2 mol of alkalinity are lost for 1 mol of inorganic carbon fixed within photosynthesis, the remaining mole being precipitated as calcite.

Alkalinity (Alk) was shown to be the main DIC source to macrophytes in a downstream reach of a river in the South of France (Maberly et al. 2015). A recent study of GPP in five US rivers (Aho et al. 2021) estimated that HCO_3^- could support up to 30% of the annual GPP in one large and sunny reach of the Connecticut River. The contribution of HCO_3^- in supporting GPP in lakes remains to be quantified, and its implications for the carbon cycle of hardwater lakes are to be understood.

Lake Geneva is a moderately hardwater lake with surface CO_2 concentrations below saturation for the stratified period. Herein, we aim at detecting the origin of the dominant DIC supporting GPP in both the pelagic and littoral environments of Lake Geneva on a daily scale. By combining hourly CO_2, O_2, and alkalinity measurements over a complete annual cycle, we categorize the dominant daily source of DIC to GPP based on the stoichiometric changes of CO_2–O_2 and Alk–O_2. We relate the DIC source to the environmental conditions to estimate the importance of HCO_3^- use for the littoral and pelagic GPP at an annual scale.

Methods

Study sites

Lake Geneva is a large, deep, alkaline hardwater lake with surface alkalinity ranging from 1200 to 1700 μeq L^{-1}, a surface calcium concentration (Ca^{2+}) ranging from 38 to 46 mg L^{-1}, and a salinity of ~0.2‰. The lake is stratified from April to September with a thermocline deepening from 3 to 30 m. Calcite precipitation occurs throughout during the stratification period (Müller et al. 2016; Escoffier et al. 2023). Two study sites (Fig. S1a–c), the LéXPLORE platform (110-m depth; Wüest et al. 2021) and the Buchillon mast (4-m depth), representative of the pelagic and littoral environments, were investigated over the years 2019 and 2020.

Field methods

Dissolved oxygen was measured by miniDOT sensors (PME). Dissolved pCO_2 was measured by miniCO$_2$ sensors (Pro-Oceanus System Inc.). Alkalinity is strongly correlated to the specific conductance over the whole year in Lake Geneva (R^2 = 0.95; Supporting Information Methods). The subdaily dynamics of alkalinity are thereby estimated using a conductivity logger (HOBO U24-001; Onset).

Local weather conditions were continuously recorded by a Campbell Scientific automatic weather station at each site. Water temperatures were measured from 0.7 to 30 m with 2.5 m of interval depth using Minilog II-T (VEMCO) in the pelagic area. These temperatures were used to compute the Schmidt stability (Idso 1973) and the mixed layer depth (Imberger 1985). Finally, all variables were gridded at an hourly time step (Perolo et al. 2022; more details about sensors and calibration in Supporting Information Methods).

Data analysis and modeling

The CO_2 and O_2 concentrations at the lake surface were expressed in terms of departure from atmospheric equilibrium in μmol L^{-1} as in Vachon et al. (2020). At the pH of Lake Geneva's surface waters (pH 7.8–9; *see* Fig. S2), HCO_3^- represents > 89% of the total alkalinity (Alk = $HCO_3^- + 2CO_3^{2-}$;

Stumm and Morgan 1981). Besides, carbonate (CO_3^{2-}) cannot be used by primary producers. We thereby assumed the Alk variations to be equal to the HCO_3^- variations (Groleau et al. 2000). The origin of the dominant DIC supporting GPP was detected from the analysis of paired CO_2–O_2 and Alk–O_2 dynamics (Stets et al. 2017; Aho et al. 2021), following an approach inspired but expanded from Vachon et al. (2020) (Fig. S3).

Briefly, the slopes of the daily point clouds of CO_2–O_2 (α) and Alk–O_2 (β; 95% confidence interval) were used to categorize the dominant source of DIC (i.e., >50% of CO_2 or HCO_3^-) supporting GPP based on the following stoichiometric ratios. The photosynthesis from CO_2 uptake leads to daily molar ratios for CO_2–O_2 between 1 : 1 and 1 : 1.4 (Lefèvre and Merlivat 2012). Daily point clouds of CO_2–O_2 with α slopes equivalent to −1 and −1.4 were categorized as days of dominant CO_2 uptake. $\alpha < -1.4$ indicates O_2 production for limited changes of CO_2 but does not necessarily evidence bicarbonate use (*see* explanation and illustration in Supporting Information Method and Fig. S5). Unambiguous demonstration of HCO_3^- use requires evidence of alkalinity consumption. For case with $\alpha < -1.4$, coupled Alk–O_2 changes were scrutinized to check whether daily alkalinity consumption matched O_2 production (Fig. S9). Direct HCO_3^- use for CCM generates a molar Alk–O_2 ratio of 1 : 1 to 1 : 1.4, while for DIC uptake from calcite precipitation, the molar Alk–O_2 ratio is expected to be lower (1 : 0.5 to 1 : 1). Daily point clouds of Alk–O_2 with β slopes between −0.5 and −1.4 were thus categorized as days of dominant HCO_3^- use. Only days with significant linear correlations between CO_2–O_2 and Alk–O_2 were retained for the analysis (i.e., $p < 0.05$ and $R^2 > 0.66$). The remaining days, not attributed to any category, are, in most cases, either days where the daily significant slopes were too weak or days with a noisy daily signal. Noisy signals can be caused by short-lived events such as internal waves or upwelling (Fernández Castro et al. 2021) produced by wind events (>5 m s^{-1}; Fig. S4).

Daily rates of GPP (μmol O_2 L^{-1} d^{-1}) were computed using a Bayesian Lake Metabolism model provided in the LakeMetabolizer R package (Winslow et al. 2016; Read et al. 2011; Supporting Information Method). We tested whether the dominant origins of DIC supporting GPP could be predicted from the four (littoral) and five (pelagic) daily averaged selected environmental variables (GPP rate, CO_2 departure, wind speed, solar radiation, and Schmidt stability) using classification trees (Supporting Information Method). The best models were used to reconstruct the dominant daily DIC sources of GPP for the not-classified days for which GPP could be computed.

Results

Spatiotemporal variability

The annual CO_2–O_2 dynamics of the littoral and pelagic environments are illustrated at an hourly resolution in Fig. 1 (time series in Fig. S6). Two distinct periods are observed in the littoral and pelagic environments (Fig. 1a,b): a cold period (September–March) corresponding to the first windy event in fall until the end of the winter mixing and a warm period (April–August) corresponding to the highest levels of solar radiation and stratification strength.

During the cold period, the conditions are mainly undersaturated in O_2 and oversaturated in CO_2. The slope of the CO_2–O_2 dynamics remains close to −1, reflecting the classical stoichiometry of photosynthesis (i.e., use of CO_2). The range of CO_2 departures is similar for the littoral and pelagic sites, while the O_2 departures are, on average, ∼30 μmol L^{-1} lower in the littoral as compared to the pelagic site.

These conditions shift to an O_2 oversaturation and a CO_2 undersaturation during the stratified period. Over these months, the slope of the CO_2–O_2 dynamic strongly deviates from −1 and becomes much steeper. This high production of O_2 and low consumption of CO_2 sheds light on the potential CO_2 limitation in this system.

The data distribution within the CO_2–O_2 diagram is more scattered for the shoulder seasons (March–April and September–October; Fig. S7), especially for the littoral site. For those shoulder months, the CO_2–O_2 variability within a single day can be almost as wide as the monthly and annual CO_2–O_2 variability (Fig. S8).

Figure 1c,d shows the results of the two processes including CO_2 uptake or HCO_3^- use for GPP. More examples are provided in Fig. S9. The distribution of DIC sources is broadly partitioned depending on O_2–CO_2 departures, with most days of CO_2 uptake at CO_2 supersaturated and O_2 undersaturated daily conditions and HCO_3^- use at CO_2 undersaturated and O_2 oversaturated conditions. However, GPP could rely on HCO_3^- use even on days with supersaturated daily averaged CO_2 values, especially in the pelagic site.

Influence of chemical and physical conditions

Figure 2 presents the relationships between the CO_2 uptake and HCO_3^- use of GPP and the daily chemical and physical conditions. Figure 2a shows a clear partition of DIC source according to GPP and average daily CO_2 departures in the littoral site with HCO_3^- use for CO_2 departures < -4.4 μmol L^{-1} and GPP > 16 μmol O_2 L^{-1} d^{-1} (classification tree for the littoral in Table S1). The physical conditions, such as wind speed, have a limited impact on DIC use (Fig. S10). In the pelagic site, the water column stability is the main driver of DIC use, followed by the GPP level, with HCO_3^- use for a Schmidt stability >116 J m^{-2} and a GPP >5 μmol O_2 L^{-1} d^{-1} (Fig. 2b and classification tree for the pelagic in Table S2). Moreover, for the highest GPP level > 50 μmol O_2 L^{-1} d^{-1}, the slopes of the CO_2–O_2 ratio tend to infinity, while the slopes of Alk–O_2 ratio align to the 1 : –1 involving an assimilation >95% of HCO_3^- to maintain these GPP levels (Fig. S9).

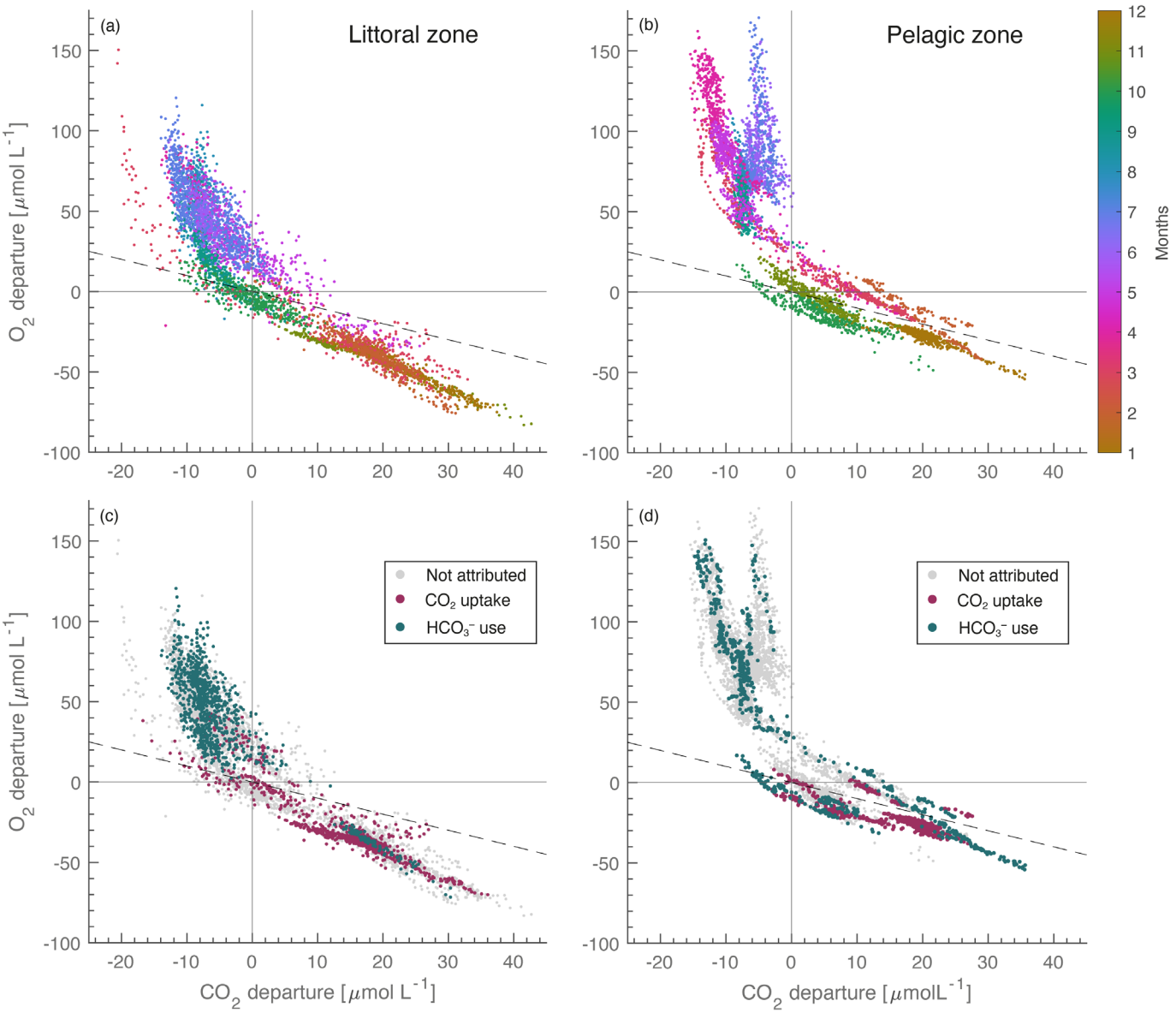

Fig. 1. Panels (**a**, **b**) show the annual dynamic of CO_2 departure vs. O_2 departure (μmol L^{-1}) in littoral and pelagic environments colored according to the months of the year. The two annual cycles present more than 65% of the days of the year distributed over all months (*see* also Fig. S4). Panels (**c**, **d**) highlight the two categorisations of CO_2 uptake (α slopes from −1 to −1.4: red points) and HCO_3^- use (α slope < −1.4 and β slopes from −0.5 to −1.4: green points) as well as the not attributed days (gray points). The dashed line represents the −1 slope.

DIC pool contribution to GPP along the year

The predictions accuracies for the classification trees are > 80% and reveal the strong predictive power of some specific drivers (i.e., CO_2 departure and GPP for the littoral environment, stability, and GPP for the pelagic environment; Tables S1, S2). Trained classification models are thereafter used to reconstruct the dominant DIC use for days that could not be categorized from their stoichiometric relationships (approximately two-thirds of the datasets). The distributions of GPP within DIC use categories are very similar between the training dataset and the predictions (*see* violin plots Before|After in Fig. 3).

In the littoral site, GPP is exclusively supported by CO_2 uptake in winter and late fall, while HCO_3^- use is the dominant source for GPP in summer (June–August), when the highest GPP rates are recorded. From March to May, GPP is alternatively supported by HCO_3^- and CO_2 because of strong daily fluctuations in CO_2 (Fig. 3a). Overall, we estimate that 75% of the total annual littoral GPP (sum of GPP with a dominant HCO_3^- source divided by sum of total GPP; from data in

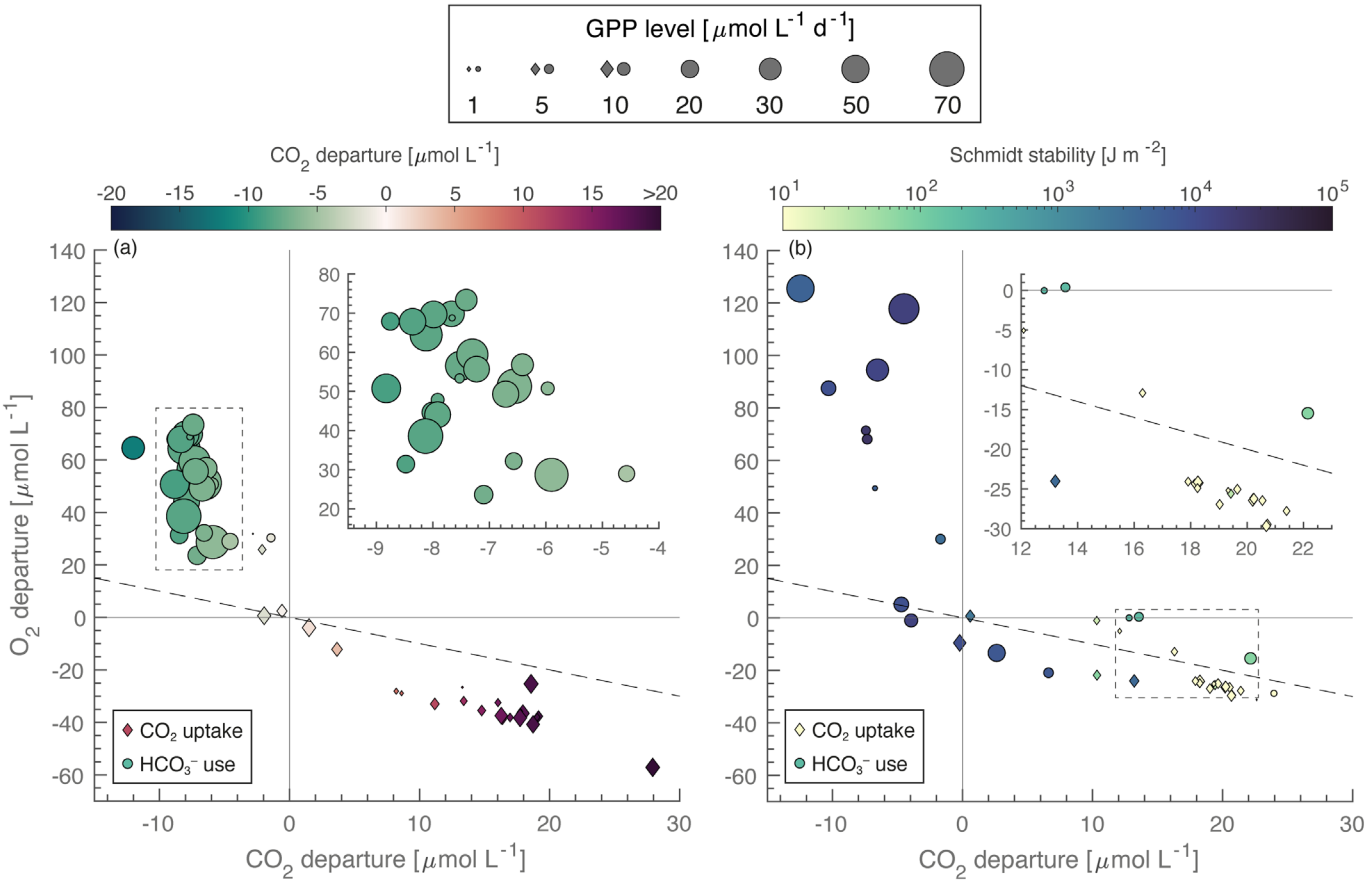

Fig. 2. Panels (**a**, **b**) show daily GPP level (size of symbol, μmol O_2 L^{-1} d^{-1}) matching categorized days for dominant CO_2 uptake (diamond) or dominant HCO_3^- use (circle). Panel (**a**) is colored according to the daily average of CO_2 departure (μmol L^{-1}) in the littoral environment. Panel (**b**) is colored according to the daily Schmidt stability (J m^{-2}) in the pelagic environment. The dashed line represents the −1 slope. Dash rectangles are the specific zooms created in the small frames in the upper right corners.

Fig. 3) occurs under dominant HCO_3^- fixation. In summer, when GPP rates are the greatest, the littoral GPP is exclusively under dominant HCO_3^- fixation.

DIC use is more seasonally partitioned for the pelagic site (Fig. 3b), with exclusive CO_2 uptake limited to winter (December–March). The dominance of HCO_3^- use starts in March and remains the main source supporting GPP over the 8 months of the thermal stratification (until October). The dominant DIC source for GPP alternated in early fall, as the water column stability fluctuated around 2000 J m^{-2}. Because HCO_3^- use dominates during the most productive season, we estimate that almost all of GPP during the stratification period occurs under dominant HCO_3^- fixation while 82% of the total annual pelagic GPP is supported by dominant HCO_3^- fixation.

Discussion

The high-frequency data coupling of CO_2, O_2, and alkalinity provides meaningful ecosystem function information (e.g., Stets et al. 2017; Vachon et al. 2020). The analyses of stoichiometric slopes allow to detect the origin of the dominant DIC supporting GPP and, complemented by the classification tree, offer an interesting and easily reproducible approach for estimating alkalinity contribution for GPP over a full year. Because the relationship between CO_2 and O_2 departures (α slope) in alkaline and hardwater lakes such Lake Geneva is nonlinear (Fig. S5c), the daily Alk–O_2 analyze (β slope) is essential to assess the dominant DIC source for daily GPP. Our method, based on stoichiometric slopes, yet provides semi-quantitative estimates. First, the GPP's substrate can shift from CO_2 to HCO_3^- within the same day (Fig. S7, S9), which limits the accuracy of our estimates. Second, the two mechanisms by which GPP can fix alkalinity differ in their stoichiometric ratios (1 : 2 for CP and 1 : 1 for CCM), affecting the expected values for the β slope. Future studied should focus on the intraday dynamics to improve the analysis of precise CO_2–HCO_3^- cofixation. Besides, microbiology and C isotopic analysis could also help disentangle CCM from

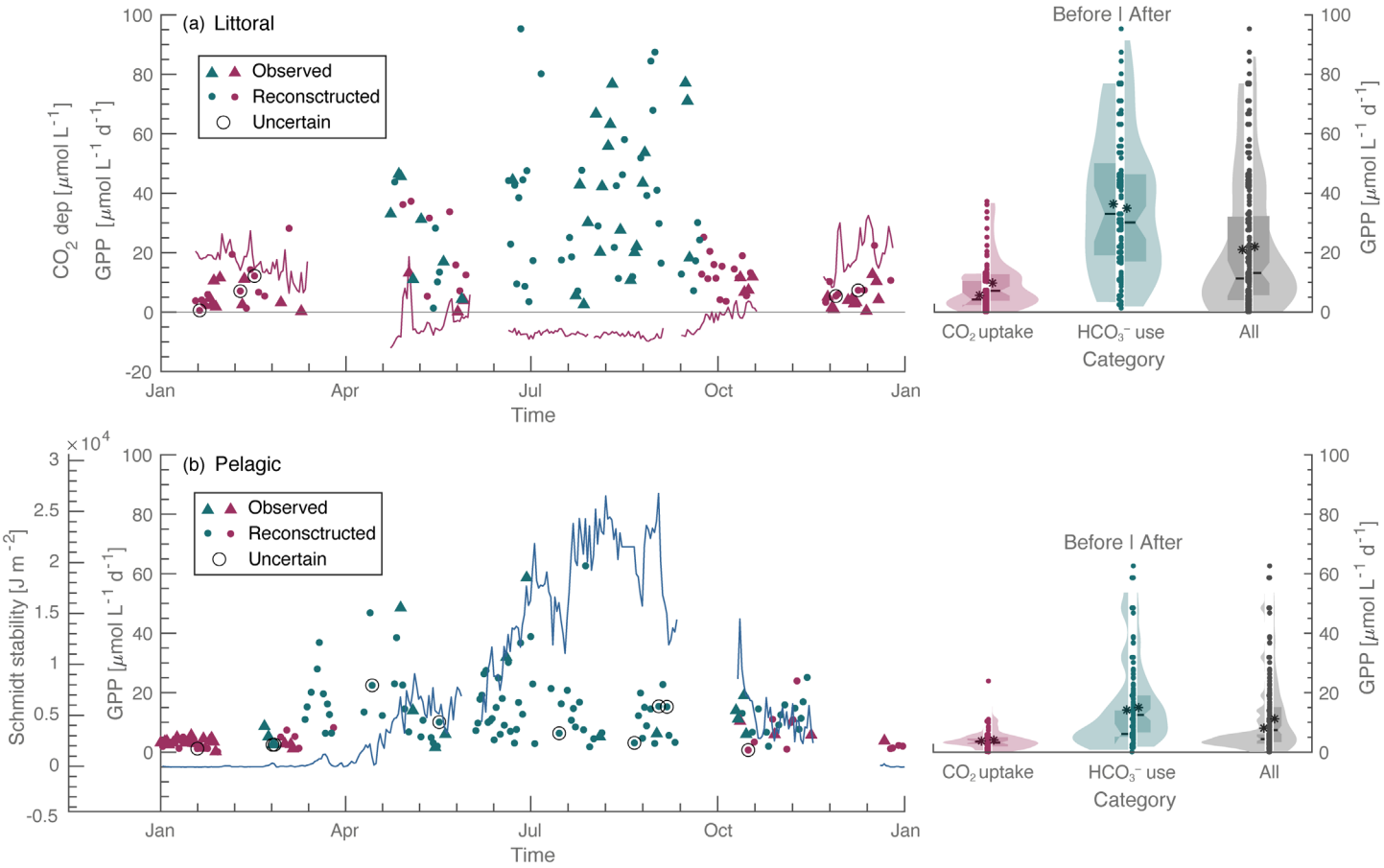

Fig. 3. Panels (**a**, **b**) show the temporal evolution of estimated GPP levels (μmol O_2 L^{-1} d^{-1}) along the year (left side) colored according to categorisations of the dominant daily DIC source: CO_2 uptake (red) and HCO_3^- use (green) and observed days (triangle) and reconstructed days (point). Circles show uncertain reconstructed days due to high wind speed > 5 m s^{-1} producing weak biological patterns. Panel (**a**) adds the temporal evolution of the CO_2 departure (μmol L^{-1}) as the best predictor of the littoral environment as well as the atmospheric equilibrium (black line). Panel (**b**) adds the temporal evolution of the Schmidt stability (J m^{-2}) as the best predictor of the pelagic environment. The distributions and the boxplots (violin plots) of GPP levels are shown on the right side of panels (**a**, **b**) for both DIC categories and the whole GPP levels before and after the reconstruction by the classification tree.

CP. Beyond their stochiometric differences, CCM, which is an active mechanism, and the supposed passive CP should differ in the induced energetic costs for primary producers (e.g., Maberly and Gontero 2017; Li et al. 2018). Whether alkalinity fixation occurred from CP or CCM might therefore have implications for GPP itself.

This study provides a semi-quantification of DIC pool contribution to GPP along an annual cycle in both the littoral and pelagic environments of a moderate alkaline and hard-water lake. The results show that GPP is not limited by carbon availability throughout the year, even during CO_2 depletion, as demonstrated in other freshwater systems (Maberly et al. 2015; Kragh and Sand-Jensen 2018; Li et al. 2018; Aho et al. 2021). To support the high rate of O_2 production, GPP relies on HCO_3^- withdrawal from the water to subsidize the missing CO_2 (Fig. S9), resulting in a depleted alkalinity pool (Fig. S6). Both lake environments are auspicious for CCM with specific conditions such as CO_2 depletion, high HCO_3^- availability and high levels of solar radiation (Maberly and Gontero 2017). Most of phytoplankton species are known to use CCM (e.g., Maberly and Gontero 2017; Mishra et al. 2018), among which picocyanobacterial that have been documented in relatively high abundances in Lake Geneva from spring to fall, when they can contribute up to 76% of the pelagic biomass of primary producers (Parvathi et al. 2014). In addition, authigenic CP, produced inorganically in the water column (Schrag et al. 2013) has previously been reported in the pelagic area (Escoffier et al. 2022; Escoffier et al. 2023; Fig. S1g). CP is also directly observed on the leaves of macrophytes from the littoral site (*Characea* and *Potamogeton perfoliatus*; Fig. S1d–f).

Exploring the temporal and spatial variabilities also offers interesting insights into macro- and micropatterns at different resolutions. At the seasonal scale, an evident temporal

variability is observed between the cold (CO_2 uptake) and warm periods (HCO_3^- use), with heterogeneity in DIC sources during the shoulder periods (Figs. 1–3). At the annual scale, the proportion of total GPP produced under dominant HCO_3^- fixation is relatively similar in the two environments (i.e., 75% for the littoral environment and 82% for the pelagic environment). These results amount to a minimum conservative estimate of HCO_3^- used for GPP over the year of 37% and 41% close to the results given by Aho et al. (2021) in the Connecticut River (~ 30%). However, this dominant consumption of HCO_3^- in the littoral environment only occurred for 3–4 months (middle June to middle September) while in the pelagic environment it was spread over 8 months (March–October). This annual similarity comes from the fact that summer littoral GPP rates are almost twice as high as in the pelagic environment. The faster CO_2 depletion in the pelagic domain can be explained by the thermal stratification isolating the epilimnion from CO_2 fluxes coming from the hypolimnion and bottom sediments. In contrast, the shallower depth in the littoral area allows for greater proximity with sediment-derived CO_2 fluxes all year round and explains that CO_2 depletion appears later when GPP levels become higher. The daily observations support such dynamics in the littoral domain with changes in slopes between morning (lower) and afternoon (steeper), illustrating the cycling of different DIC sources. In contrast, the pelagic slopes stay linear and steeper all day (Figs. S7, S9). These daily patterns also highlight a greater dynamic from the littoral environment during the shoulder period with a constant return to early morning conditions (Fig. S7). In contrast, the pelagic environment has greater inertia, as observed in March, where the daily cycle of the littoral is the same as the monthly cycle in the pelagic (Fig. S8), linked to an increase in the Schmidt stability (Fig. 3).

To conclude, this study, as several recent studies (Maberly et al. 2015; Stets et al. 2017; Kragh and Sand-Jensen 2018; Khan et al. 2020; Aho et al. 2021), sheds light on the overlooked role of alkalinity in the freshwater carbon cycle and how it contributes to GPP. Half of the world's lakes are considered alkaline (> 1 meq L^{-1}; Marcé et al. 2015), so we can expect alkalinity consumption by primary producers to be a widespread phenomenon. Moreover, alkalinity consumption by GPP might get more frequent with climate warming. Longer and stronger stratification and shallower mixing depths (Schwefel et al. 2016; Gaudard et al. 2017) would both fasten surface CO_2 depletion during stratification and limit winter replenishment of surface CO_2. Therefore, less CO_2 at the surface could lead to a potential increase in HCO_3^- use and a shift in species communities capable of such an assimilation.

References

Aho, K. S., J. D. Hosen, L. A. Logozzo, W. R. McGillis, and P. A. Raymond. 2021. Highest rates of gross primary productivity maintained despite CO_2 depletion in a temperate river network. Limnol. Oceanogr.: Lett. **6**: 200–206. doi:10.1002/lol2.10195

Bade, D. L., and J. J. Cole. 2006. Impact of chemically enhanced diffusion on dissolved inorganic carbon stable isotopes in a fertilised lake. J. Geophys. Res.: Oceans **111**: C01014. doi:10.1029/2004JC002684

Cole, J. J., N. F. Caraco, G. W. Kling, and T. K. Kratz. 1994. Carbon dioxide supersaturation in the surface waters of lakes. Science **265**: 1568–1570. doi:10.1126/science.265.5178.1568

Colman, B., I. E. Huertas, S. Bhatti, and J. S. Dason. 2002. The diversity of inorganic carbon acquisition mechanisms in eukaryotic microalgae. Funct. Plant Biol. **29**: 261. doi:10.1071/PP01184

Dillon, P. J., and F. H. Rigler. 1974. The phosphorus-chlorophyll relationship in lakes. Limnol. Oceanogr. **19**: 767–773. doi:10.4319/lo.1974.19.5.0767

Fernández Castro, B., H. E. Chmiel, C. Minaudo, S. Krishna, P. Perolo, S. Rasconi, and A. Wüest. 2021. Primary and net ecosystem production in a large lake diagnosed from high-resolution oxygen measurements. Water Resour. Res. **57**. doi:10.1029/2020WR029283

Escoffier, N., P. Perolo, T. Lambert, J. Rüegg, D. Odermatt, T. Adatte, T. Vennemann, and M.-E. Perga. 2022. Whiting events in a large peri-alpine lake: Evidence of a catchment-scale process. J. Geophys. Res.: Biogeosciences **127**: e2022JG006823. doi:10.1029/2022JG006823

Escoffier, N., P. Perolo, G. Many, N. Pasche, and M.-E. Perga. 2023. Unveiling the fine scale dynamics of calcite precipitation in a large hardwater lake. Sci. Total Environ. **864**: 160699. doi:10.1016/j.scitotenv.2022.160699

Finlay, K., M. E. Power, and G. Cabana. 1999. Effect of water velocity on algal carbon isotope ratios: Implications for river food web studies. Limnol. Oceanogr. **44**: 1198–1203. doi:10.4319/lo.1999.44.5.1198

Gaudard, A., R. Schwefel, L. R. Vinnå, M. Schmid, A. Wüest, and D. Bouffard. 2017. Optimising the parameterisation of deep mixing and internal seiches in one-dimensional hydrodynamic models: A case study with Simstrat v1.3. Geosci. Model Dev. **10**: 3411–3423. doi:10.5194/gmd-10-3411-2017

Groleau, A., G. Sarazin, B. Vinçon-Leite, B. Tassin, and C. Quiblier-Llobéras. 2000. Tracing calcite precipitation with specific conductance in a hard water alpine lake (Lake Bourget). Water Res. **34**: 4151–4160. doi:10.1016/S0043-1354(00)00191-3

Idso, S. B. 1973. On the concept of lake stability. Limnol. Oceanogr. **18**: 681–683. doi:10.4319/lo.1973.18.4.0681

Imberger, J. 1985. The diurnal mixed layer. Limnol. Oceanogr. **30**: 737–770. doi:10.4319/lo.1985.30.4.0737

Iversen, L. L., and others. 2019. Catchment properties and the photosynthetic trait composition of freshwater plant communities. Science **366**: 878–881. doi:10.1126/science.aay5945

Karlsson, J., P. Byström, J. Ask, P. Ask, L. Persson, and M. Jansson. 2009. Light limitation of nutrient-poor lake ecosystems. Nature **460**: 506–509. doi:10.1038/nature08179

Kelts, K., and K. J. Hsü. 1978. Freshwater carbonate sedimentation, p. 295–323. *In* A. Lerman [ed.], *Lakes*. Springer. doi:10.1007/978-1-4757-1152-3_9

Khan, H., A. Laas, R. Marcé, and B. Obrador. 2020. Major effects of alkalinity on the relationship between metabolism and dissolved inorganic carbon dynamics in lakes. Ecosystems **23**: 1566–1580. doi:10.1007/s10021-020-00488-6

Kragh, T., and K. Sand-Jensen. 2018. Carbon limitation of lake productivity. Proc. R. Soc., Ser. B **285**: 20181415. doi:10.1098/rspb.2018.1415

Krause-Jensen, D., and K. Sand-Jensen. 1998. Light attenuation and photosynthesis of aquatic plant communities. Limnol. Oceanogr. **43**: 396–407. doi:10.4319/lo.1998.43.3.0396

Larsson, C., and L. Axelsson. 1999. Bicarbonate uptake and utilization in marine macroalgae. Eur. J. Phycol. **34**: 79–86. doi:10.1080/09670269910001736112

Lefèvre, N., and L. Merlivat. 2012. Carbon and oxygen net community production in THE eastern tropical Atlantic estimated from a moored buoy. Glob. Biogeochem. Cycles **26**: GB1009. doi:10.1029/2010GB004018

Li, H., Y. Wu, and L. Zhao. 2018. Effects of carbon anhydrase on utilisation of bicarbonate in microalgae: A case study in Lake Hongfeng. Acta Geochim. **37**: 519–525. doi:10.1007/s11631-018-0277-4

Maberly, S. C., and B. Gontero. 2017. Ecological imperatives for aquatic CO_2-concentrating mechanisms. J. Exp. Bot. **68**: 3797–3814. doi:10.1093/jxb/erx201

Maberly, S. C., S. A. Berthelot, A. W. Stott, and B. Gontero. 2015. Adaptation by macrophytes to inorganic carbon down a river with naturally variable concentrations of CO_2. J. Plant Physiol. **172**: 120–127. doi:10.1016/j.jplph.2014.07.025

Marcé, R., B. Obrador, J.-A. Morguí, J. Lluís Riera, P. López, P, and J. Armengol 2015. Carbonate weathering as a driver of CO2 supersaturation in lakes. Nature Geoscience **8**: 107–111. doi:10.1038/ngeo2341

Mishra, S., B. Joshi, P. Dey, H. Pathak, and A. Kohra. 2018. CCM in photosynthetic bacteria and marine alga. J. Pharmacogn. Phytochem. **7**: 928–937. doi:10.22271/phyto/2018.7692

Müller, B., J. S. Meyer, and R. Gächter. 2016. Alkalinity regulation in calcium carbonate-buffered lakes. Limnol. Oceanogr. **61**: 341–352. doi:10.1002/lno.10213

Parvathi, A., X. Zhong, A. S. Pradeep Ram, and S. Jacquet. 2014. Dynamics of auto- and heterotrophic picoplankton and associated viruses in Lake Geneva. Hydrol. Earth Syst. Sci. **18**: 1073–1087. doi:10.5194/hess-18-1073-2014

Pełechaty, M., A. Pukacz, K. Apolinarska, A. Pełechata, and M. Siepak. 2013. The significance of Chara vegetation in the precipitation of lacustrine calcium carbonate. Sedimentology **60**: 1017–1035. doi:10.1111/sed.12020

Perolo, P., N. Escoffier, and H. E. Chmiel. 2022. CO_2, O_2, and alkalinity in Lake Geneva. Zenodo. doi:10.5281/zenodo.7442327

Price, G. D., M. R. Badger, F. J. Woodger, and B. M. Long. 2008. Advances in understanding the cyanobacterial CO_2-concentrating-mechanism (CCM): Functional components, Ci transporters, diversity, genetic regulation and prospects for engineering into plants. J. Exp. Bot. **59**: 1441–1461. doi:10.1093/jxb/erm112

Read, J. S., D. P. Hamilton, I. D. Jones, K. Muraoka, L. A. Winslow, R. Kroiss, C. H. Wu, and E. Gaiser. 2011. Derivation of lake mixing and stratification indices from high-resolution lake buoy data. Environ. Model. Softw. **26**: 1325–1336. doi:10.1016/j.envsoft.2011.05.006

Schindler, D. W. 1971. Carbon, nitrogen, and phosphorus and the eutrophication of freshwater lakes. J. Phycol. **7**: 321–329. doi:10.1111/j.1529-8817.1971.tb01527.x

Schindler, D. W. 1974. Eutrophication and recovery in experimental lakes: Implications for lake management. Science **184**: 897–899. doi:10.1126/science.184.4139.897

Schindler, D. W., G. Brunskill, S. Emerson, W. Broecker, and T.-H. Peng. 1972. Atmospheric carbon dioxide: Its role in maintaining phytoplankton standing crops. Science **177**: 1192–1194. doi:10.1126/science.177.4055.1192

Schindler, D. W., H. Kling, R. V. Schmidt, J. Prokopowich, V. E. Frost, R. A. Reid, and M. Capel. 1973. Eutrophication of Lake 227 by addition of phosphate and nitrate: The second, third, and fourth years of enrichment, 1970, 1971, and 1972. J. Fish. Res. Board Can. **30**: 1415–1440. doi:10.1139/f73-233

Schrag, D. P., J. A. Higgins, F. A. MacDonald, and D. T. Johnston. 2013. Authigenic carbonate and the history of the global carbon cycle. Science **339**: 540–543. doi:10.1126/science.1229578

Schwefel, R., A. Gaudard, A. Wüest, and D. Bouffard. 2016. Effects of climate change on deepwater oxygen and winter mixing in a deep lake (Lake Geneva): Comparing observational findings and modeling. Water Resour. Res. **52**: 8811–8826. doi:10.1002/2016WR019194

Steemann Nielsen, E. 1946. Carbon sources in the photosynthesis of aquatic plants. Nature **158**: 594–596. doi:10.1038/158594a0

Stets, E. G., D. Butman, C. P. McDonald, S. M. Stackpoole, M. D. DeGrandpre, and R. G. Striegl. 2017. Carbonate buffering and metabolic controls on carbon dioxide in rivers: Controls on CO_2 in rivers. Glob. Biogeochem. Cycles **31**: 663–677. doi:10.1002/2016GB005578

Stumm, W., and J. J. Morgan. 1981, *Aquatic chemistry: An introduction emphasising chemical equilibria in natural waters*, 2nd Edition. Wiley.

Thomas, E. A., and E. B. Tregunna. 1968. Bicarbonate ion assimilation in photosynthesis by *Sargassum muticum*. Can. J. Bot. **46**: 411–415. doi:10.1139/b68-063

Vachon, D., and others. 2020. Paired O_2–CO_2 measurements provide emergent insights into aquatic ecosystem function. Limnol. Oceanogr.: Lett. **5**: 287–294. doi:10.1002/lol2.10135

Wanninkhof, R., and M. Knox. 1996. Chemical enhancement of CO_2 exchange in natural waters. Limnol. Oceanogr. **41**: 689–697. doi:10.4319/lo.1996.41.4.0689

Winslow, L. A., J. A. Zwart, R. D. Batt, H. A. Dugan, R. I. Woolway, J. R. Corman, P. C. Hanson, and J. S. Read. 2016. LakeMetabolizer: An R package for estimating lake metabolism from free-water oxygen using diverse statistical models. Inland Waters **6**: 622–636. doi:10.1080/IW-6.4.883

Wüest, A., D. Bouffard, J. Guillard, B. W. Ibelings, S. Lavanchy, M.-E. Perga, and N. Pasche. 2021. LéXPLORE: A floating laboratory on Lake Geneva offering unique lake research opportunities. WIREs Water **8**: e1544. doi:10.1002/wat2.1544

Zagarese, H. E., and others. 2021. Patterns of CO_2 concentration and inorganic carbon limitation of phytoplankton biomass in agriculturally eutrophic lakes. Water Res. **190**: 116715. doi:10.1016/j.watres.2020.116715

Zhang, T., and others. 2017. River sequesters atmospheric carbon and limits the CO_2 degassing in karst area, Southwest China. Sci. Total Environ. **609**: 92–101. doi:10.1016/j.scitotenv.2017.07.143

Acknowledgment

We would like to thank the entire team of the LéXPLORE platform for their administrative and technical support and the LéXPLORE core dataset. We also acknowledge the five partner institutions involved with LéXPLORE: Eawag, EPFL, the University of Geneva, the University of Lausanne, and CARRTEL (INRAE-USMB). This study was supported by the CARBOGEN project (SNF 200021_175530), which is linked to the LéXPLORE project (SNF R'Equip, P157779) and the Primary Production Under Oligotrophication in Lakes project (SNF 200021_179123). The authors thank Sébastien Lavanchy, the chief technical officer (APHYS-EPFL), and Aurélien Ballu, a member of the technical pool (IDYST-UNIL) of LéXPLORE platform, for their technical and field support. In addition, we thank Prof Yves Prairie (University of Québec à Montréal) and Prof Anne Ojala (University of Helsinki) for their reading of the manuscript and their constructive comment.

Submitted 06 April 2022
Revised 11 January 2023
Accepted 16 January 2023